Seeking enhanced lead/acid battery performance through the use of conductive tin-dioxide-coated glass-flakes

L.T. Lam, O. Lim, H. Ozgun and D.A.J. Rand
CSIRO Division of Mineral Products, P.O. Box 124, Port Melbourne, Vic. 3207 (Australia)

Abstract

The aim of this research is to raise the level of active-material utilization in the positive plates of lead/acid batteries (without diminishing other performance characteristics) and, thereby, to increase the energy output per unit weight. The strategy is to increase the electrical conductivity of the material by adding a proprietary particulate that consists of glass-flakes coated with a thin (<5 μm) layer of tin dioxide. The particulates are incorporated in positive plates that are prepared as automotive designs under a wide range of processing conditions, i.e., paste densities, acid-to-oxide ratios, low-/high-temperature (3BS/4BS) curing. Plate performance is evaluated in terms of active-material utilization, cold-cranking capability, repetitive reserve capacity, and life endurance under the Japanese Industrial Standard (JIS) procedure. Compared with untreated cells, the following benefits of adding the particulates to positive plates have been confirmed: (i) acceleration of the formation process; (ii) increase in the BET surface area of formed materials; (iii) improvement in active-material utilization at the 5-h and 20-h discharge rates; (iv) maintenance of cycleability under repetitive, reserve-capacity duty; (v) increase in cycle life under the JIS schedule. The encouraging outcomes of this research suggest that further benefits are likely to be gained by designing elongated particulates of lighter weight. This will increase the number of counts per unit area and, thereby, will improve the contact between the individual particles of the positive active material and will further enhance the electrical conductivity of the plate.

Breaking the energy barrier

Despite worldwide efforts over the past three decades to develop new types of rechargeable batteries, the lead/acid system continues to be the principal choice for energy-storage devices that require substantial power levels. Given the fact, however, that established and emerging markets are forcing increasing levels of performance from rechargeable batteries, major improvements in lead/acid technology must be achieved if the battery is to maintain its pre-eminent position. The key advancement to be made in more demanding applications (such as electric vehicles and portable power supplies) is higher specific energy.

The specific energy is the number of watt-hours of electricity that the battery can deliver per kilogram of its mass for a nominated rate of discharge. For any given battery system, a maximum value for this parameter is easily calculated; it is the product of the cell potential (in volts), the number of electrons involved in the cell reaction and the electronic charge (in ampere-hours), divided by the sum of the weights (in kilograms) of the moles of the reactants that take part in the reaction. Practical specific energies, however, are well below the theoretical maxima. Apart from electrode

0378-7753/94/$07.00
SSDI 0378-7753(93)01860-K

kinetic and other restrictions that serve to reduce the cell voltage and prevent full utilization of the reactants, there is a need for construction materials that add to the battery weight but are not involved in the energy-producing reaction. These materials are required for current collectors, separators, connectors, terminals and the battery container, for instance.

Seeking improvements in specific energy through an increase in the use of the reactants (the so-callel 'active materials') and/or a decrease in the weight of the inert structural materials presents special problems in the case of the lead/acid battery. Apart from the obvious weight penalty imposed by the high specific gravity of lead and its compounds, the battery suffers from a particularly low utilization of active material in the positive plate. This limitation in performance is promoted by two factors: (i) slow diffusion of sulfuric acid from the bulk of the solution into the interior of the plates; (ii) continuous decrease in the conductivity of the positive and negative plates during discharge. The discharge problems become more acute as the discharge rate is increased. In electric-vehicle operations, for example, only about 20 to 30% of the positive active material can be accessed to provide electrical energy.

During discharge, the positive active material is composed of lead dioxide (PbO_2) crystals that have the following two functions: (i) to participate in the electrochemical reaction, that is the conversion of PbO_2 to $PbSO_4$; (ii) to act as electron pathways from each reaction-site in the porous active mass to the grid; this non-reacting material provides structure and conductivity to the plate, but does not contribute to the reaction. As discharge of the plate proceeds, the conductivity decreases as a result of the formation of increasing amounts of lead sulfate ($PbSO_4$). In some locations, areas of PbO_2 can become encapsulated by the non-conductive $PbSO_4$ so that no further reaction can take place, even if large numbers of PbO_2 crystals and sufficient sulfuric acid solution are present in the inner parts of the $PbSO_4$ capsules. This is because the electron pathway, as well as the flow of solution reactants through the pores of the active mass, are both hindered by the $PbSO_4$. This situation is shown schematically by area A in Fig. 1.

Increasing the porosity of the plate is an obvious approach to reducing the incidence of $PbSO_4$ encapsulation. This has encouraged numerous studies of the influence of the plate-processing stages on the morphology of the active material, and how the growth and distribution of crystals during these stages result in material unavailability. The use of low paste densities has been attempted, but this tends to reduce cycle

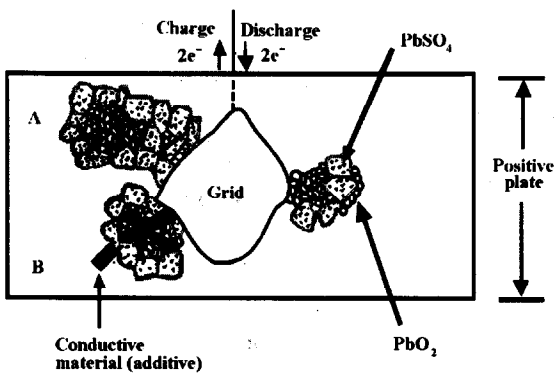

Fig. 1. Schematic illustration of the cross section of a lead/acid positive plate during discharge in the presence/absence of a conductive additive.

life through weakening of both the mechanical strength and the corrosion resistance of the plates. The incorporation of additives that either promote porosity (e.g., carboxymethyl cellulose [1], carbon black [1], graphite [2, 3], glass microspheres [4]) or favourably modify crystal size (e.g., silica gel [1]) has also been investigated. Except for the glass microspheres, all the materials tested to date undergo oxidative attack and, consequently, any gains in plate performance are not lasting [1].

The use of an electrically conducting additive is the alternative approach to overcoming the insulating effects of $PbSO_4$. If a conductive material can be deployed in such a manner that it connects regions of isolated PbO_2 with their reactive neighbours (and, thus, with the grid), the discharge reaction can proceed at the otherwise inactive locations and the degree of active-material utilization will be increased, see area B, Fig. 1. Doubtless, a wide range of prospective conductive additives has been examined in house by battery manufacturers. The list reported in the literature, however, is surprisingly short, namely: carbon fibres [5]; barium metaplumbate [6]; titanium sub-oxides, Ti_nO_{2n-1} [7]. This fact has also been noted by other authors [2].

The work presented here describes an evaluation of a proprietary additive — a tin-dioxide-coated glass-flake — that aims to improve paste conductivity and, consequently, to raise active-material utilization. The additive has been developed by the Monsanto Chemical Company (St Louis, USA) from technology originally introduced by ENSCI, Inc. (Santa Monica, USA), see ref. 8. The experimental strategy has involved a successive determination of the effects of two different forms of the additive (particulates A and B) on the active-material utilization, the cold-cranking performance, and the cycle life (under standard schedules) of positive plates in practical battery cells. The plates have been made under a variety of processing conditions, i.e., paste densities, acid-to-oxide paste ratios, high-/low-temperature curing.

Experimental strategy

An overview of the experimental programme that was employed to prepare untreated and doped plates, and to evaluate their performance in cells, is given in Table 1. The plates were of an NS40 automotive design.

Plate preparation

Pastes were prepared according to four different formulae, denoted as I to IV. These formulae yielded two paste densities, namely, 3.9 g cm^{-3} for pastes I and II, and 3.5 g cm^{-3} for pastes III and IV. Two acid-to-oxide ratios were employed for each paste density, i.e., 6.6% (for pastes I and III) and 3.9% (for pastes II and IV). For the doped pastes, tin-dioxide-coated glass-flakes (particulates A and B, see Table 1) were added to the leady oxide at the 2 wt.% level and the resulting mixture was shaken thoroughly in a container before addition to the paste mixer.

The plates were pasted by hand in the laboratory. In order to minimize possible inconsistencies between different operators, the pastes were applied evenly to Pb–1.7wt.% Sb grids with a polyvinyl chloride (PVC) plate, and were then compacted under the weight (5 kg) of a purpose-built, stainless-steel roller.

After pasting, the plates were mounted vertically in a stainless-steel rack in which adjacent plates were allowed to touch in order to simulate the curing conditions commonly encountered in commercial battery manufacture. The rack was placed in a petri dish that contained a small amount of distilled water, and the total assembly was enclosed by a large beaker. Curing was performed at either 50 or 90 °C, with

TABLE 1

Conditions of plate preparation and sequential experimental programme for evaluating the effects of tin-dioxide-coated additives

Curing method	Additive[a]		Paste type[b]			
	type	(wt.%)	I	II	III	IV
4BS	A	0	1[c]	2	3	4
		2.0	9	10	11	12
	B	2.0	13	14	15	16
3BS	A	0	5	6	7	8
		2.0	17	18	19	20
	B	2.0	21	22	23	24

[a]Particulate A = 1/64 inch glass-flake with a 0.3 μm (nominal) thick coating of tin dioxide. Particulate B = 1/8 inch glass-flake with a 0.3 μm (nominal) thick coating of tin dioxide.
Note: particulates A and B are produced by different coating processes; 4BS = tetrabasic lead sulfate ($4PbO \cdot PbSO_4$); 3BS = tribasic lead sulfate ($3PbO \cdot PbSO_4 \cdot H_2O$).

[b]Past type	acid-to-oxide ratio (%)	paste density (g cm^{-3})
I	6.6	3.9
II	3.9	3.9
III	6.6	3.5
IV	3.9	3.5

[c]Numbers 1 to 24 denote the order in which the experiments were conducted.

95% relative humidity (r.h.), for 48 h. The plates were then dried at 75 °C until the moisture content fell to below 0.1 wt.%. It was found that the vertical racking arrangement preserved good uniformity of temperature and, consequently, it was confirmed that the plate phase composition was consistent throughout each batch.

The cured plates were grouped into 2-V cells that each consisted of four positives (enclosed in Daramic envelope separators) and five negatives. The negative plates were produced under factory conditions. Sulfuric acid solution (1.235 sp. gr.) was introduced and a constant current of 5 A was applied for 20 h at 20 °C. After formation, the specific gravity of the acid was increased to about 1.270 sp. gr.

Characterization of materials

Samples of leady oxide, and pasted, cured and formed materials were subjected to X-ray diffraction (XRD) phase analysis through the use of techniques developed in the CSIRO laboratories [9, 10]. The morphology of the same materials, as well as cycled materials, was examined with a JEOL JSM-25S III scanning electron microscope (SEM) [9]. The surface areas of samples of leady oxide and formed materials were obtained by the BET method [11] that involved the adsorption of a mixture of nitrogen and helium (30% N_2 and 70% He) at the temperature of liquid nitrogen. The adsorption measurements were carried out on a continuous-flow Quantachrome (Model Monosorb) instrument. The porosity and pore volume of the formed material was determined [11] by mercury intrusion porosimetry with a Micromeritics Model 9200 instrument.

Evaluation of cell performance

After formation, each cell was kept at open circuit for 15 min at 25 °C. A constant current of 2.5 A was applied until the terminal voltage and acid density exhibited no appreciable change (i.e., within ±3%) between three, consecutive, hourly readings. This condition was taken as the fully-charged state of the cell and was achieved prior to each measurement of performance.

Discharge capacity

After full charging, the acid density in each cell was adjusted to lie between 1.265 and 1.275 g cm^{-3} at 25 °C. The cell was then discharged at a constant current of 5.5 A (5-h rate) or 1.7 A (20-h rate) and a measurement was made of the taken time for the terminal voltage to fall to 1.75 V. The product of the current and the time is the discharge capacity. The procedure was repeated for 3 or 4 times until the measured capacity reached a maximum value.

Cold-cranking capability

The Australian Standard procedure [12] was applied. The cells were placed in a refrigerator until the temperature of the electrolyte reached -18 ± 1 °C. Discharge was then conducted at three different currents: one close to, and one on either side of, the specified cold-cranking value. The terminal voltage at the end of 5 and 30 s was recorded.

Repetitive reserve capacity

The cell temperature was maintained at 25 °C and the acid density was adjusted to lie between 1.265 and 1.275 g cm^{-3}. The cell was discharged at 25 A until the terminal voltage fell to 1.75 V. The time, in min, taken for the terminal voltage to fall to 1.75 V is the rated reserve capacity. The test was repeated until the measured reserve capacity was equal to 20 min.

Japanese Industrial Standard (JIS) endurance cycling

The cell was kept at 40 to 45 °C, discharged at 10 A for 1 h, and charged at 2.5 A for 5 h. This discharge/charge schedule is equivalent to '1 cycle' [13]. At each successive set of 25 cycles, the cell was discharged at 10 A until the terminal voltage reached 1.75 V. The duration of the discharge was recorded. Failure was taken as the point at which the capacity fell to 50%, or less, of the nominal 5-h capacity.

For each test, the values of the charge and discharge currents were based on the 5-h discharge capacity of the cell. The JIS test conditions state that the discharge and charge currents shall be 50% of the respective specified values for cells having a 5-h capacity of 72 Ah or less, and shall be 25% of the specified values for cells of 24 Ah or less. The 5-h capacity of the cells examined here is 27 Ah. Since this is very close to the test changeover value, the cells were discharged and charged at 25% of the respective specified currents.

Results and discussion

Characterization of conductive glass-flake

X-ray diffraction phase analysis clearly demonstrated that the coating consists predominantly of tin dioxide; any other phase, if indeed present, would exist in only minor amounts because the minimum detection limit of the phase analysis technique is about 2 wt.%.

Electron micrographs of particulates A (Fig. 2(a), (b)) and B (Fig. 2(c), (d)) clearly reveal that the surface of the tin dioxide film is not smooth. At high magnification, it can be seen that the film consists of individual grains. The latter are smaller for particulate B. At some locations, the glass-flake substrate is exposed and this suggests that the coverage by tin dioxide could be improved.

Back-scattered electron micrographs of the cross sections of particulates A and B are presented in Fig. 3(a) and (c), respectively. The conductive film has an uneven thickness that varies between 0.5 and 5 μm. The values in this range are significantly different from the nominal thickness of 0.3 μm. The corresponding tin maps (Fig. 3(b), (d)), obtained by energy dispersive spectrometric (EDS) analysis, again demonstrate that some parts of the surfaces of the glass-flakes are not covered by the tin dioxide film (e.g., regions highlighted by white arrows in Fig. 3(c), (d)).

The chemical stability of the glass-flakes was determined by placing 2 g of each particulate in 30 ml of H_2SO_4 solution (1.275 sp. gr.) at 20 °C, to simulate battery conditions. The amount of tin leached into the solution was monitored weekly by atomic absorption spectrometric analysis. The results are shown in Fig. 4. During the first two weeks of exposure to acid, tin is leached at a steady rate from particulate A to give a total dissolved amount of ~2.5 mg. Thereafter, the particulate appears to be immune to acid attack. The limiting value of dissolved tin is ~7.5% of the total amount present in the sample. The conductive layer on particulate B is more stable; the total amount of dissolved tin reaches a limiting value of only ~0.6 mg after two weeks, i.e., ~1.4% of the total tin in the sample.

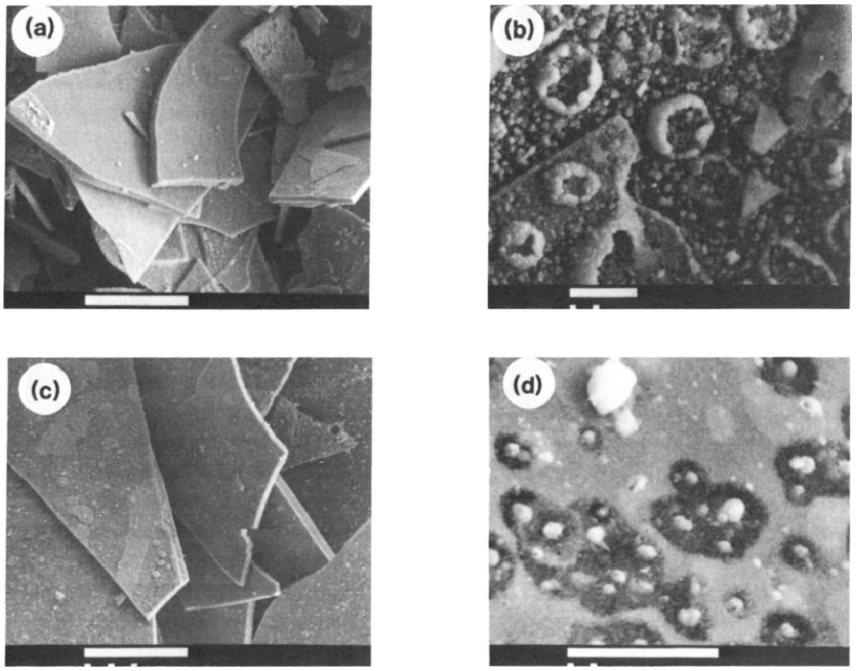

Fig. 2. Electron micrographs of conductive glass-flakes (a), (b) particulate A; (c), (d) particulate B. Magnification bar: (a), (c) 100 μm; (b), (d) 10 μm.

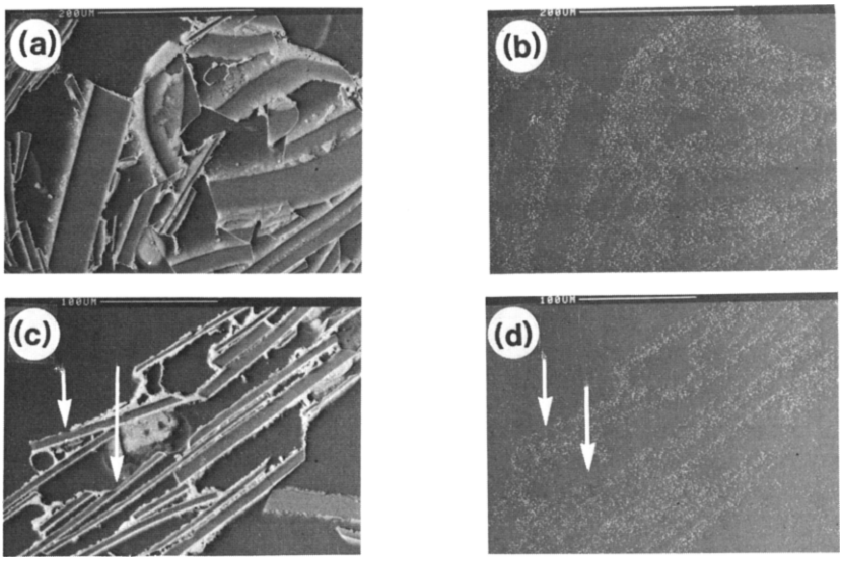

Fig. 3. Back-scattered electron micrographs and energy dispersive spectroscopy tin maps of conductive glass-flakes: (a), (b) particulate A; (c), (d) particulate B. Magnification bar: (a), (b) 200 μm; (c), (d) 100 μm.

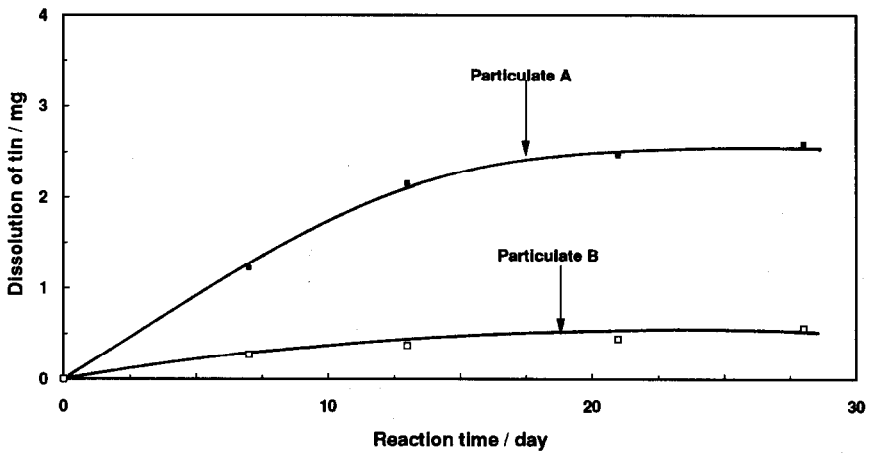

Fig. 4. Amount of tin leached from conductive glass-flakes on exposure to battery acid (1.275 sp. gr.).

In summary, the above results show that: (i) the conductive layer of both particulates A and B is comprised predominantly of tin dioxide; (ii) there is scope to improve the uniformity of the layer coverage; (iii) the layer on particulate B has smaller grains and higher stability in acid.

Characterization of paste materials

Phase-analysis data for pastes with/without the addition of 2 wt.% of particulate A or B are given in Table 2. No major differences in phase composition exist between

TABLE 2

Phase analysis (wt.%) of paste materials

Experiment number[a]	Additive (2 wt.%)	Phase composition				
		Pb	α-PbO	β-PbO	3BS	1BS[b]
Paste I: acid-to-oxide ratio = 6.6%; density = 3.9 g cm^{-3}						
1, 5		8	38	10	41	3
9, 17	A	10	29	16	45	
13, 21	B	8	37	11	37	7
Paste II: acid-to-oxide ratio = 3.9%; density = 3.9 g cm^{-3}						
2, 6		9	69		20	2
10, 18	A	11	57	7	22	3
14, 22	B	10	60	4	22	4
Paste III: acid-to-oxide ratio = 6.6%; density = 3.5 g cm^{-3}						
3, 7		10	36	10	40	4
11, 19	A	14	26	9	46	5
15, 23	B	10	34	13	39	4
Paste IV: acid-to-oxide ratio = 3.9%; density = 3.5 g cm^{-3}						
4, 8		12	63		22	3
12, 20	A	16	54	7	21	2
16, 24	B	11	55	8	23	3

[a]See Table 1.

[b]1BS = $PbO \cdot PbSO_4$. Note: the starting oxide contains 27 wt.% Pb; 66 wt.% α-PbO; 7 wt.% β-PbO.

the untreated and doped pastes produced from the same paste type. This indicates that: (i) tin-dioxide-coated glass-flakes exert little influence on the phase composition; (ii) the pastes are produced with good consistency. Similarly, a change in paste density gives rise to no major differences in paste composition. By contrast, the acid-to-oxide ratio exerts a significant effect on the paste composition. The level of tribasic lead sulfate (3BS) decreases with decrease in the ratio from 6.6 to 3.9%. This is due to the fact that, at the lower ratio, less acid is available to react with the lead oxide during mixing. Most of the pastes contain minor amounts of monobasic lead sulfate (1BS). This material is harmful to plate strength and, therefore, to battery life. In the present case, however, the relatively small amounts of 1BS produced in the paste are unlikely to cause any serious impediment to plate performance.

SEM revealed that the morphology of untreated pastes produced with the same paste density, but different acid-to-oxide ratios, is similar. The grain size of the needle-like 3BS crystals is smaller in the high-ratio paste. This also holds (but to a lesser extent) for pastes containing conductive glass-flakes. There is little difference in either the morphology or the size of the 3BS crystals in untreated and doped pastes produced from the same acid-to-oxide ratio.

In summary, the above studies show that the addition of tin-dioxide-coated glass-flakes imposes little change to either the phase composition or the morphology/grain-size of the paste. The acid-to-oxide ratio, however, influences both the level and the crystal size of the 3BS in the paste. The yield of 3BS is greater, and the size is smaller, when a high ratio is used.

Characterization of cured materials

Phase-analysis data for the cured materials produced under conditions of either 50 °C/high r.h. or 90 °C/high r.h. are given in Table 3. The phase composition of untreated and doped materials after curing at 50 °C is close to that of the precursor paste (cf., data in Table 2), except for a decrease in the content of free lead (due to the further oxidation of this material). In experiment 22, however, the cured material contains an abnormally low 3BS level, viz., 8 wt.% compared with 22 wt.% in the paste. When untreated plates are cured at 90 °C, the levels of both free lead and α-PbO decrease from those in the paste, while the 3BS content disappears due to the formation of tetrabasic lead sulfate (4BS). Under the same curing conditions, most of the doped plates retain appreciable amounts of 3BS in addition to 4BS.

Material (with/without particulate) cured at 50 °C consists of tiny, needle-like, 3BS crystals. With all other parameters kept constant, the size of these crystals is slightly smaller in doped plates. SEM examination of polished cross sections of the

TABLE 3

Phase analysis (wt.%) of cured materials

Experimental conditions	Phase composition					
	Pb	α-PbO	β-PbO	3BS	4BS	1BS
Paste I: acid-to-oxide ratio = 6.6%; density = 3.9 g cm^{-3}						
5, 3BS, untreated	3	34	15	45		3
17, 3BS, A	3	20	26	51		
21, 3BS, B	4	26	18	46		6
1, 4BS, untreated	2	23	10		65	
9, 4BS, A	2	15	2		81	
13, 4BS, B	5	13	14	25	37	6
Paste II: acid-to-oxide ratio = 3.9%; density = 3.9 g cm^{-3}						
6, 3BS, untreated	3	73		24		
18, 3BS, A	5	55	17	19		4
22, 3BS, B	5	83	4	8		
2, 4BS, untreated	3	62			35	
10, 4BS, A	3	44	15	2	36	
14, 4BS, B	4	41	12	7	36	
Paste III: acid-to-oxide ratio = 6.6%; density = 3.5 g cm^{-3}						
7, 3BS, untreated	5	33	17	45		
19, 3BS, A	2	23	24	46		5
23, 3BS, B	3	23	23	46		5
3, 4BS, untreated	3	10	14		73	
11, 4BS, A	3	17	16	22	37	5
15, 4BS, B	2	14	10	11	63	
Paste IV: acid-to-oxide ratio = 3.9%; density = 3.5 g cm^{-3}						
8, 3BS, untreated	2	71	2	25		
20, 3BS, A	3	52	18	24		3
24, 3BS, B	3	56	15	23		3
4, 4BS, untreated	2	47			49	
12, 4BS, A	3	39	15	9	34	
16, 4BS, B	3	35	12		46	4

cured plates reveal that there is good contact between the active material and the mildly corroded grid member. The size of the 3BS crystals in untreated and doped plates is smaller in cured plates prepared from paste with a high acid-to-oxide ratio. This trend is consistent with that found for 3BS development during paste mixing. The active material appears to adhere securely to the conductive glass-flakes under all plate-processing conditions.

The high-temperature cured material prepared from a paste with a high acid-to-oxide ratio contains large, rectilinear, 4BS crystals. Although the 4BS crystals prepared from doped and untreated pastes do not display any noticeable differences in morphology, the size of the crystals is smaller in plates that contain the conductive glass-flakes. This indicates that the additive exerts an influence on the nucleation and growth of the 4BS crystals. As with low-temperature cured materials, there is a good contact between the active material and, individually, both the grid and the glass-flakes. In fact, through SEM examination, it was found that 4BS crystals can develop from the

TABLE 4

Phase analysis (wt.%) of formed materials

Experimental conditions	Phase composition				
	α-PbO	β-PbO	β-PbO_2	$PbSO_4$	4BS
Paste I: acid-to-oxide ratio = 6.6%; density = 3.9 g cm^{-3}					
5, 3BS, untreated			48	52	
17, 3BS, A		4	83	13	
21, 3BS, B			78	22	
1, 4BS, untreated			13	87	
9, 4BS, A		6	31	19	44
13, 4BS, B		14	39	29	18
Paste II: acid-to-oxide ratio = 3.9%; density = 3.9 g cm^{-3}					
6, 3BS, untreated	26		62	12	
18, 3BS, A	5		75	20	
22, 3BS, B	4		74	22	
2, 4BS, untreated	39		22	21	18
10, 4BS, A	24		27	33	16
14, 4BS, B	18		36	31	15
Paste III: acid-to-oxide ratio = 6.6%; density = 3.5 g cm^{-3}					
7, 3BS, untreated			84	16	
19, 3BS, A		2	83	15	
23, 3BS, B			72	28	
3, 4BS, untreated	6		18	56	20
11, 4BS, A			56	37	7
15, 4BS, B	10	5	23	50	12
Paste IV: acid-to-oxide ratio = 3.9%; density = 3.5 g cm^{-3}					
8, 3BS, untreated	21		52	27	
20, 3BS, A	23		55	22	
24, 3BS, B	29		55	16	
4, 4BS, untreated	33		28	29	10
12, 4BS, A	25	6	23	46	
16, 4BS, B	26	7	18	49	

TABLE 5

BET surface area (± 0.05 m^2 g^{-1}) of untreated and doped formed materials

Experimental conditions	Additive	Curing temperature (°C)	BET surface area (m^2 g^{-1})
Paste I: acid-to-oxide ratio = 6.6%; density = 3.9 g cm^{-3}			
5		50	7.84
17	A	50	8.02
21	B	50	9.60
1		90	5.06
9	A	90	6.31
13	B	90	8.67
Paste II: acid-to-oxide ratio = 3.9%; density = 3.9 g cm^{-3}			
6		50	6.07
18	A	50	7.64
22	B	50	6.91
2		90	3.71
10	A	90	3.95
14	B	90	3.79
Paste III: acid-to-oxide ratio = 6.6%; density = 3.5 g cm^{-3}			
7		50	9.96
19	A	50	9.91
23	B	50	10.36
3		90	5.87
11	A	90	6.86
15	B	90	7.87
Paste IV: acid-to-oxide ratio = 3.9%; density = 3.5 g cm^{-3}			
8		50	8.31
20	A	50	9.09
24	B	50	9.52
4		90	5.45
12	A	90	8.41
16	B	90	5.19

surface of the conductive glass-flakes. These phenomena are also observed for high-temperature cured materials prepared from paste with a low acid-to-oxide ratio, except that the size of the 4BS crystals is smaller. This effect of acid-to-oxide ratio on 4BS size is the reverse of that witnessed above for 3BS-based plate material.

Characterization of formed materials

Phase-analysis data for the formed materials produced from different experiments are given in Table 4. The formed plates produced from 4BS-rich material still contain relatively high levels of either PbO and $PbSO_4$ (paste IV) or PbO, $PbSO_4$ and 4BS (pastes I to III). This indicates that 4BS-cured plates are difficult to form, even after a period of 20 h. Such behaviour is well known. In general, the amount of β-PbO_2 in either 3BS- or 4BS-formed plates that contain conductive glass-flakes is higher than that in the untreated plates. Thus, the particulate appears to be of particular benefit in assisting the plate-formation process.

The formed plates produced under 50 °C curing conditions, with or without glass-flakes, exhibit similar morphology. The material consists of large, shapeless agglomerates

of individual crystals in the form of tiny anhedral grains. By contrast, the inherent interlocking structure of the 4BS-cured plates is not destroyed completely during the subsequent formation stage. The surface of the 4BS is converted into a large number of fine PbO_2 crystals, but the interior of the 4BS remains unoxidized. In both cases (3BS and 4BS), unconverted $PbSO_4$ particles remain in the active mass. Examination of polished cross sections of formed plates produced via the 3BS- or 4BS-curing process reveals that there is a strong bonding between the active material and the grid member. There is also good contact between the conductive glass-flake and the active material. Indeed, the formed material is able to develop from the surface of the glass-flake itself.

The BET surface-area data for formed materials prepared from untreated and doped pastes are presented in Table 5, and shown schematically in Fig. 5. For the same paste density, the surface areas of both 3BS- and 4BS-based materials decrease with decrease in the acid-to-oxide ratio. Furthermore, for the same acid-to-oxide ratio, the surface area of both 3BS- and 4BS-based materials increases with decrease in the paste density. In all cases, the surface area of a formed plate containing conductive glass-flake is larger than that of an untreated counterpart, for both low- and high-temperature curing procedures.

The pore characteristics of the formed materials produced from untreated and doped pastes are given in Table 6, and are presented schematically in Fig. 6. For formed plates derived from both untreated and doped 4BS-cured plates, the percentage of pores (i.e., the porosity) and the total pore volume are both lower than those for the 3BS counterparts, except in the case of plates made from paste IV. The latter plates exhibit the reverse effect. The doped plates prepared from pastes I to III give equal, or lower, porosity and total pore volume than the untreated varieties. By contrast, these two parameters have higher values in the doped plates produced with paste IV (see Fig. 6(a), (b)).

In general, two kinds of pores exist in formed plates — macropores and micropores [14, 15]. Macropores contribute mainly to the pore volume and provide a pathway by which reaction species can be transported from the bulk of the solution to the reactive sites. Micropores provide high surface area for the electrochemical reactions to proceed during charge and discharge. The classification of pores into micropores and macropores can be determined from measurements of the effect of pore diameter on the total pore volume and surface area (Fig. 7). For the plates prepared here, it is found that

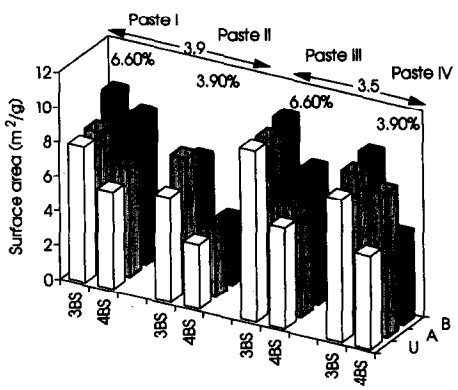

Fig. 5. Schematic representation of change in specific surface area of formed material prepared under various process conditions; U denotes untreated paste.

TABLE 6

Porosity of formed materials produced from untreated and doped pastes

Experimental conditions	Additive	Curing temperature (°C)	Porosity (%)	Total pore volume ($cm^3\ g^{-1}$)	Macropore volume ($cm^3\ g^{-1}$)
Paste I: acid-to-oxide ratio = 6.6%; density = 3.9 g cm^{-3}					
5		50	48	0.136	0.083
17	A	50	42	0.121	0.070
21	B	50			
1		90	33	0.093	0.069
9	A	90	40	0.111	0.092
13	B	90			
Paste II: acid-to-oxide ratio = 3.9%; density = 3.9 g cm^{-3}					
6		50	44	0.115	0.074
18	A	50	40	0.098	0.054
22	B	50	41	0.099	0.068
2		90	38	0.097	0.081
10	A	90	35	0.096	0.064
14	B	90	31	0.080	0.062
Paste III: acid-to-oxide ratio = 6.6%; density = 3.5 g cm^{-3}					
7		50	50	0.152	0.094
19	A	50	50	0.160	0.099
23	B	50	50	0.152	0.086
3		90	42	0.140	0.112
11	A	90	48	0.152	0.095
15	B	90	42	0.134	0.097
Paste IV: acid-to-oxide ratio = 3.9%; density = 3.5 g cm^{-3}					
8		50	37	0.094	0.051
20	A	50	40	0.115	0.060
24	B	50	45	0.143	0.070
4		90	40	0.108	0.081
12	A	90	43	0.143	0.092
16	B	90	44	0.163	0.135

pores with diameters >0.1 μm contribute mainly to the pore volume, while pores with diameters <0.1 μm provide most of the surface area. For example, at a pore diameter of 0.1 μm, the pore volume of the formed plates is about 65%, but the pore surface area is only about 13% of the respective maximum value. Therefore, pores with diameter >0.1 μm can be considered to be macropores, and those with diameter <0.1 μm to be micropores.

The volume provided by the macropores in each formed plate is presented in Table 6. In general, this volume is larger for plates derived from 4BS-cured material. This is because the formed plate still retains the open/interlocking structure of the 4BS-cured plate. As observed for the total pore volume, the volume given by the macropores is smaller for the doped plates than for the untreated plates, except in the case of plates produced from paste IV (see Fig. 6(c)).

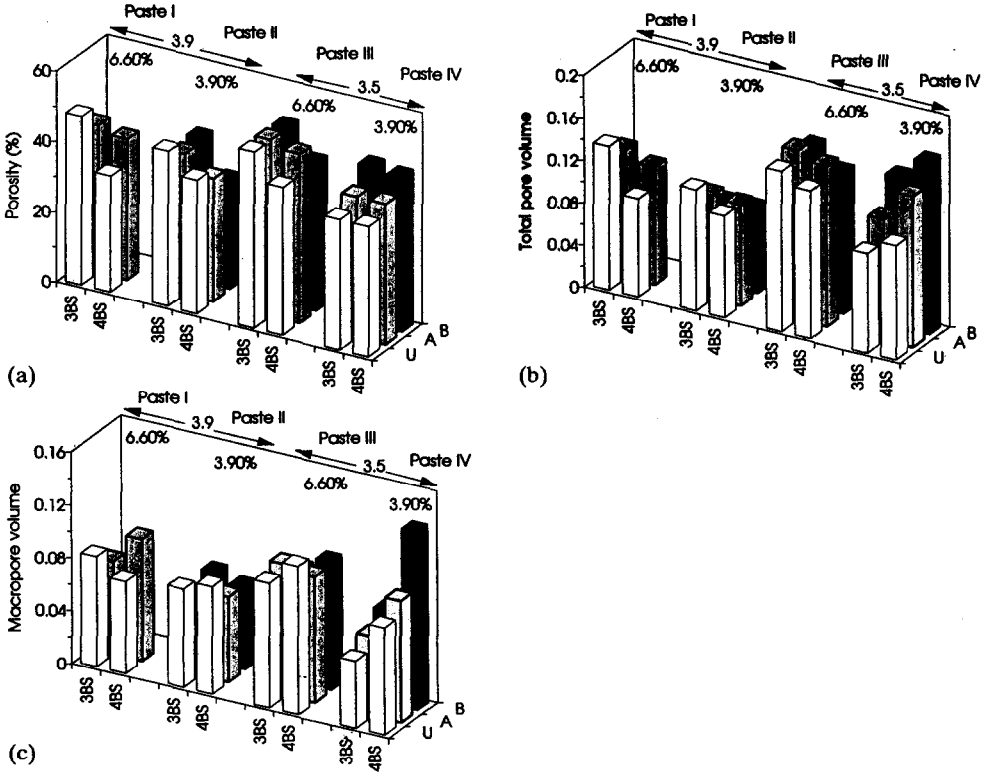

Fig. 6. Schematic representation of change in (a) porosity, (b) total pore volume, and (c) macropore volume of formed material prepared under various process conditions; U denotes untreated paste.

Summary of active-material characterization

From the above studies of the physicochemical properties of the positive active material, the following conclusions can be drawn.

- During paste mixing and curing of both treated and untreated plates, the acid-to-oxide ratio is the main determinant of both the size and the yield of either 3BS (paste-mixing/curing) or 4BS (curing). The levels of 3BS and 4BS both increase, the size of 3BS decreases, and the size of 4BS increases when employing a high acid-to-oxide ratio. These features are summarized in Table 7.
- For a given high or low acid-to-oxide ratio, the addition of tin-dioxide-coated glass-flakes exerts little influence on either the morphology or the phase composition of the 3BS paste. It does, however, modify the nucleation and growth of 4BS crystals during the curing process, i.e., the crystal size is decreased. There are irregular changes in the yield of 4BS. The overall behaviour is summarized in Table 8.
- A strong interlock is created between the active material and the conductive glass-flake, and this is maintained during the subsequent curing and formation stages.
- The addition of tin-dioxide-coated glass-flakes facilitates the plate-formation process for both 3BS- and 4BS-cured plates.
- In the presence of tin-dioxide-coated glass-flakes, the surface area of the formed plates is increased. By contrast, the porosity and total pore volume are both decreased

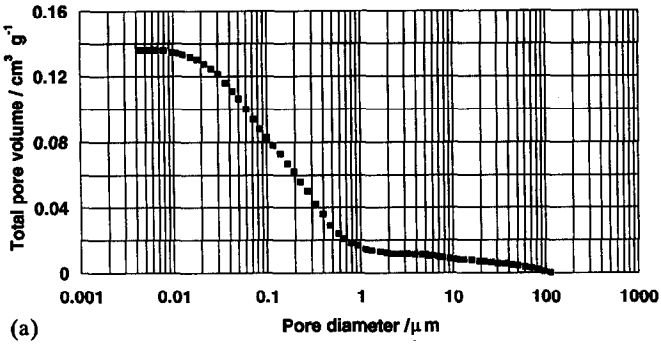

(a)

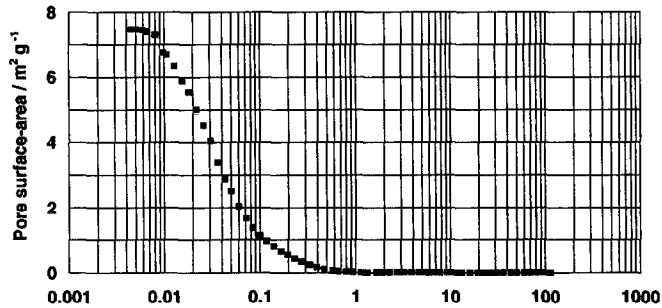

(b)

Fig. 7. Distribution of (a) cumulative pore volume and (b) pore surface area in a formed plate prepared from experiment 5; 50 °C cure; acid-to-oxide ratio = 6.6%.

TABLE 7

Effects of acid-to-oxide ratio (both paste densities) on size/yield of 3BS- and 4BS-based materials

Untreated/doped material	Acid-to-oxide ratio	
	High (6.6%)	Low (3.9%)
Paste mixing and curing		
3BS-based		
size	small	large
yield	high	low
Curing		
4BS-based		
size	large	small
yield	high	low

– except in plates using a low paste density and a low acid-to-oxide ratio, where enhanced values for these two material characteristics are observed.

Active-material utilization

Active-material utilization is defined as the ratio (%) between the measured capacity, at a particular rate of discharge, and the theoretical capacity. In other words,

TABLE 8

Relative effects of conductive glass-flakes on size/yield of 3BS- and 4BS-based materials at a given acid-to-oxide ratio

Plate material	Untreated → doped	Untreated → doped
	Size	Yield
Paste mixing and curing		
3BS-based	no effect	no effect
Curing		
4BS-based	smaller	irregular change

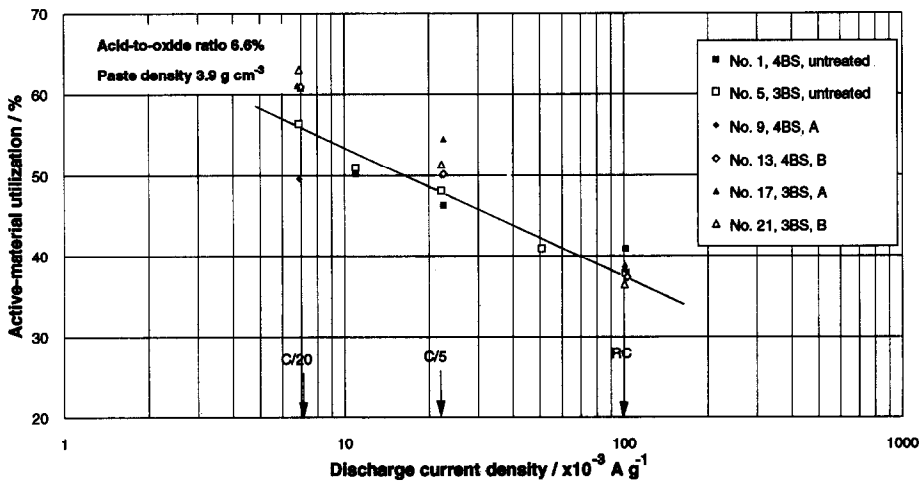

Fig. 8. Active-material utilization in cells prepared from paste I.

the parameter represents the percentage of the plate material that participates in the discharge process. The theoretical capacity is equivalent to discharging the total amount of PbO_2 in the formed plates to $PbSO_4$ at 100% efficiency. The value is calculated to be 0.229 Ah per gram of cured material.

The active-material utilization in positive plates produced from pastes I to IV is shown in Figs. 8 to 11, respectively, and is presented schematically in Fig. 12. In the former plots, the solid lines indicate the active-material utilization in cells using untreated 3BS-cured plates. As expected, the material utilization of both untreated and doped cells decreases as the rate of discharge is increased from 20 h to the reserve capacity value (i.e., 0.8 h in this study). This is due to the rapid blockage of pores by $PbSO_4$ at the higher rate.

For the same paste density of 3.9 g cm^{-3}, the level of material utilization in the untreated 3BS and 4BS cells, at the 20-h and 5-h rates, increases when the acid-to-oxide ratio is decreased from 6.6 to 3.9%. At an acid-to-oxide ratio of 6.6% (Fig. 8), the doped cells give significantly higher active-material utilization than the untreated cells at both the 20-h and 5-h rates. At an acid-to-oxide ratio of 3.9% (Fig. 9), the doped cells exhibit nearly the same material utilization as untreated cells at the

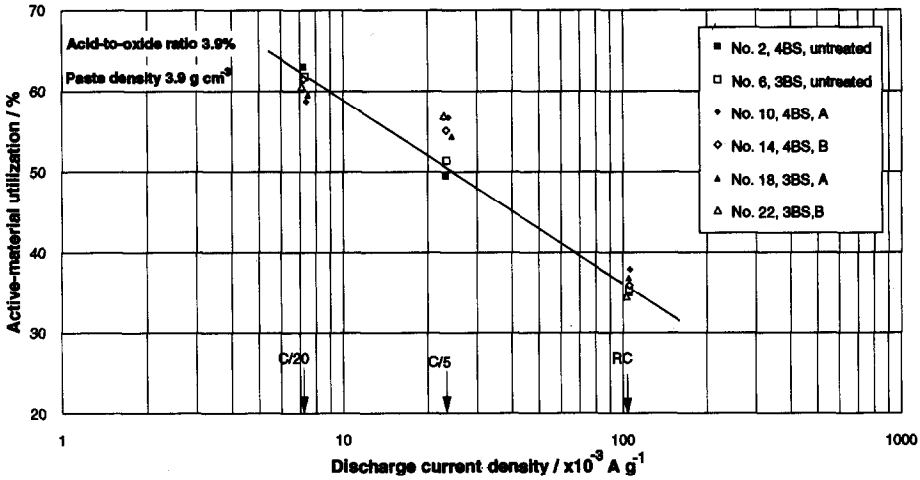

Fig. 9. Active-material utilization in cells prepared from paste II.

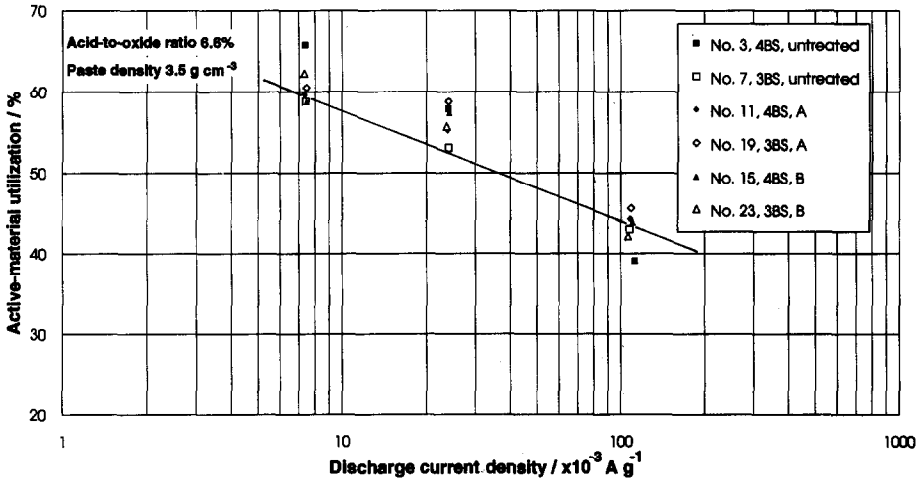

Fig. 10. Active-material utilization in cells prepared from paste III.

20-h discharge rate, but higher values at the 5-h rate. At both ratios, the conductive glass-flakes yield no major improvement at the reserve-capacity rate.

By contrast, for a paste density of 3.5 g cm^{-3}, the level of material utilization in the untreated 3BS- and 4BS-cells decreases with decrease of the acid-to-oxide ratio, even at the reserve capacity rate (cf., Fig. 10 with Fig. 11). For both acid-to-oxide ratios (6.6 and 3.9%), most of the cells containing conductive glass-flakes give higher material utilization than the untreated varieties (Fig. 12).

For an acid-to-oxide ratio of 6.6%, i.e., that used in automotive plates, a decrease in paste density results in an increase in the level of material utilization at both low and high rates of discharge (cf., Fig. 8 with Fig. 10). Conversely, for an acid-to-oxide ratio of 3.9%, a decrease in the paste density produces a corresponding decrease in

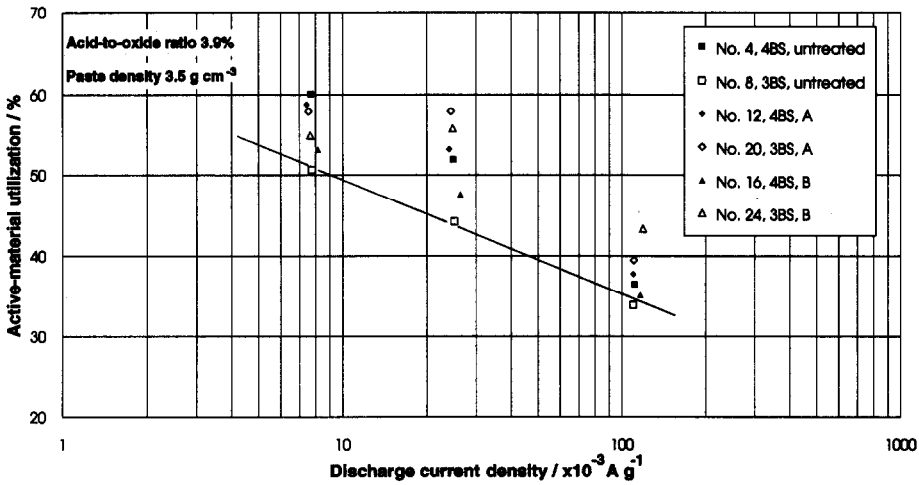

Fig. 11. Active-material utilization in cells prepared from paste IV.

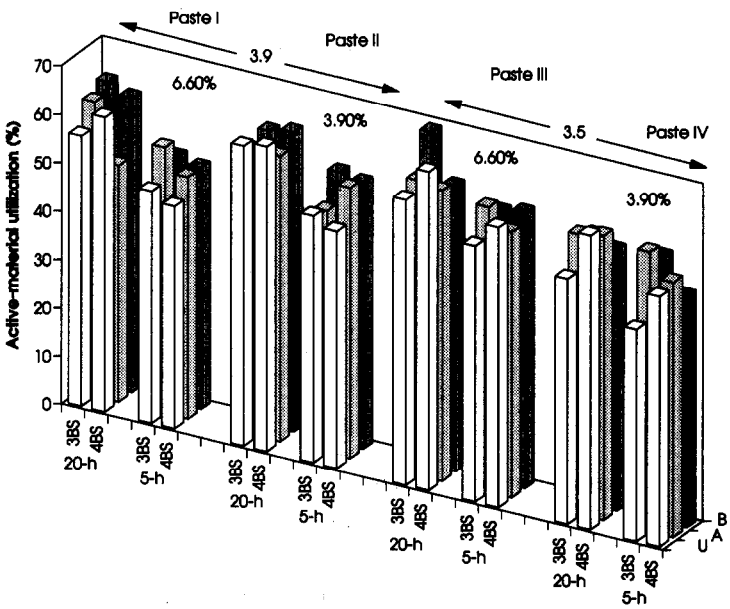

Fig. 12. Schematic representation of active-material utilization of positive-plate material (prepared under various conditions) at the 20-h and 5-h discharge rates; U denotes untreated paste.

the level of material utilization, especially for cells prepared from untreated 3BS-cured plates at the 5-h and 20-h discharge rates (cf., Fig. 9 with Fig. 11).

In order to compare the improvement in active-material utilization of the doped cells, the data are normalized to the performance of untreated cells using 3BS-cured plates because this is the usual technology for automotive batteries. The results are given in Table 9. For a paste density of 3.9 g cm^{-3} (pastes I and II), the addition of conductive glass-flakes to the positive paste promotes an increase in active-material

TABLE 9

Relative improvement in active-material utilization for untreated and doped cells

Experimental conditions	Improvement in active-material utilization (%)		
	20-h rate	5-h rate	RC rate*
Paste I: acid-to-oxide ratio = 6.6%; density = 3.9 g cm^{-3}			
5, 3BS, untreated	100	100	100
17, 3BS, A	108	114	103
21, 3BS, B	112	107	96
1, 4BS, untreated	108	96	108
9, 4BS, A	88	104	103
13, 4BS, B	108	104	99
Paste II: acid-to-oxide ratio = 3.9%; density = 3.9 g cm^{-3}			
6, 3BS, untreated	100	100	100
18, 3BS, A	96	106	104
22, 3BS, B	98	111	97
2, 4BS, untreated	102	96	99
10, 4BS, A	95	110	107
14, 4BS, B	100	107	101
Paste III: acid-to-oxide ratio = 6.6%; density = 3.5 g cm^{-3}			
7, 3BS, untreated	100	100	100
19, 3BS, A	103	111	106
23, 3BS, B	117	105	98
3, 4BS, untreated	112	109	91
11, 4BS, A	102	104	103
15, 4BS, B	100	108	102
Paste IV: acid-to-oxide ratio = 3.9%; density = 3.5 g cm^{-3}			
8, 3BS, untreated	100	100	100
20, 3BS, A	114	131	117
24, 3BS, B	109	126	128
4, 4BS, untreated	119	117	108
12, 4BS, A	116	120	112
16, 4BS, B	105	108	104

*RC = reserve capacity.

utilization of ~4 to 14% at both the 20-h and 5-h rates of discharge. By contrast, at a lower paste density of 3.5 g cm^{-3}, the doped cells display significant improvements in material utilization, namely: ~2 to 31%. The cells prepared from untreated 4BS-cured plates, using pastes III and IV, also give an increase in material utilization, i.e., ~9 to 19%.

Given that the use of conductive glass-flakes increases the active-material utilization in positive plates at the 20-h and 5-h rates, the next stage is to determine whether, or not, this improvement is due to the observed increase in BET surface area (Table 5), or to the change in pore volume (Table 6). The relationship between the active-material utilization and either the surface area or the pore volume of plates made from pastes II and III is shown in Fig. 13(a) and (b), respectively. The results demonstrate emphatically that the material utilization does not depend on either of these two parameters. These observations are also true for plates produced from the

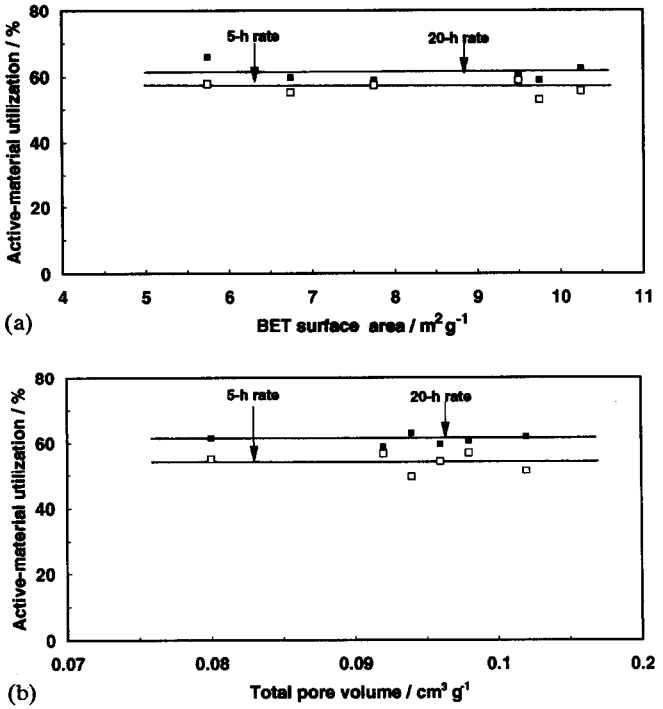

Fig. 13. Dependence of active-material utilization on (a) BET surface area, and (b) total pore volume; pastes II and III.

other two paste formulations. Thus, it is concluded that the increase in material utilization in doped cells is due to an increase in plate conductivity.

Cold-cranking performance

In test cells (four positives and five negatives) subject to cold-cranking discharge, the potential of the negative plates reaches the cutoff value before that of the positives, even though the total weight of negative material is greater than that of the positive material. This behaviour is due to the much lower surface area of the negative plate compared with that of the positive plate (i.e., 2 to 3 $m^2\ g^{-1}$ versus 6 to 10 $m^2\ g^{-1}$). In another words, the cold-cranking discharge is 'negative potential limited'.

Although not a practical design, a cell assembly that consisted of two positives and five negatives was used for the determination of the cold-cranking current under positive-potential-limited conditions. This allowed an evaluation of the effect of adding conductive glass-flakes to the positive-plate material. The results show (Table 10) that there is little difference in cold-cranking performance between the untreated and doped cells. Thus, even under positive-potential limitation, conductive glass-flakes do not enhance cold-cranking capability.

Repetitive reserve capacity

The repetitive reserve capacity of cells prepared from pastes I to IV are presented in Figs. 14 to 17, and summarized schematically in Fig. 18. A cell is considered to have failed when a reserve capacity of 20 min cannot be maintained. For both untreated

TABLE 10

SAE cold-cranking performance of cells (given as voltage reading at 5 and 30 s of discharge)

Experimental conditions	Discharge current per four positive plates					
	240 A		270 A		300 A	
	5 s	30 s	5 s	30 s	5 s	30 s
Paste II: acid-to-oxide ratio = 3.9%; density = 3.9 g cm^{-3}						
6, 3BS, untreated	1.40	1.35	1.38	1.33	1.24	0.76
18, 3BS, A	1.35	1.25	1.38	1.31	1.24	0.90
22, 3BS, B	1.37	1.28	1.32	1.15	1.25	0.60
2, 4BS, untreated	1.37	1.30	1.32	1.22	1.25	1.13
10, 4BS, A	1.38	1.33	1.40	1.33	1.24	1.13
14, 4BS, B	1.42	1.35	1.33	1.24	1.23	0.93
Paste III: acid-to-oxide ratio = 6.6%; density = 3.5 g cm^{-3}						
7, 3BS, untreated	1.45	1.40	1.26	1.15	1.23	0.98
19, 3BS, A	1.44	1.39	1.38	1.32	1.26	1.14
23, 3BS, B	1.39	1.33	1.33	1.20	1.16	0.95
3, 4BS, untreated						
11, 4BS, A	1.34	1.28	1.28	1.20	1.17	0.98
15, 4BS, B	1.46	1.43	1.32	1.25	1.29	1.20
Paste IV: acid-to-oxide ratio = 3.9%; density = 3.5 g cm^{-3}						
8, 3BS, untreated	1.36	1.30	1.31	1.22	1.29	1.14
20, 3BS, A	1.40	1.36	1.25	1.12	1.28	1.18
24, 3BS, B	1.43	1.38	1.30	1.22	1.28	1.19
4, 4BS, untreated	1.40	1.33	1.28	1.16	1.28	1.13
12, 4BS, A	1.41	1.35	1.27	1.17	1.28	1.19
16, 4BS, B	1.39	1.33	1.32	1.23	1.23	1.10

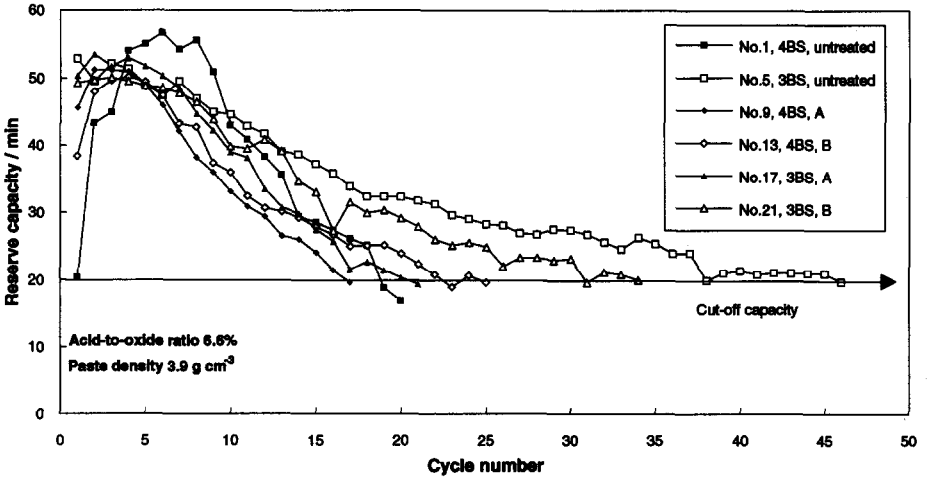

Fig. 14. Repetitive reserve capacity of cells prepared from paste I.

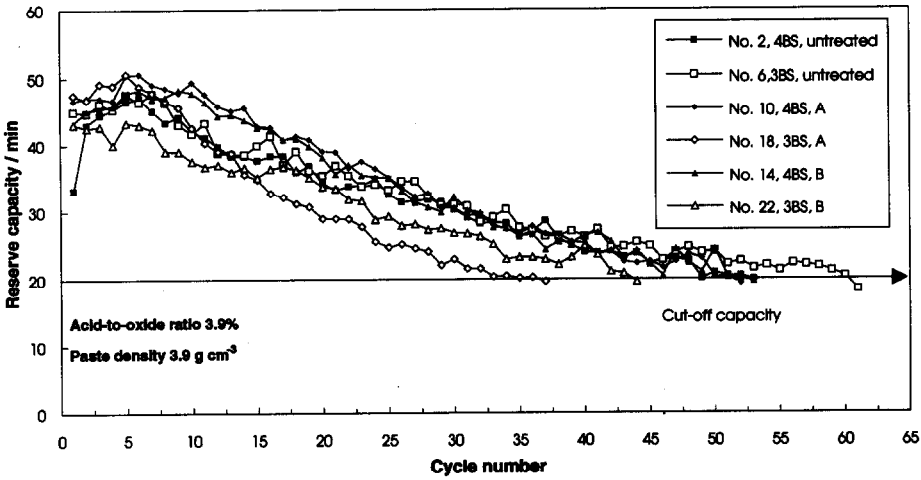

Fig. 15. Repetitive reserve capacity of cells prepared from paste II.

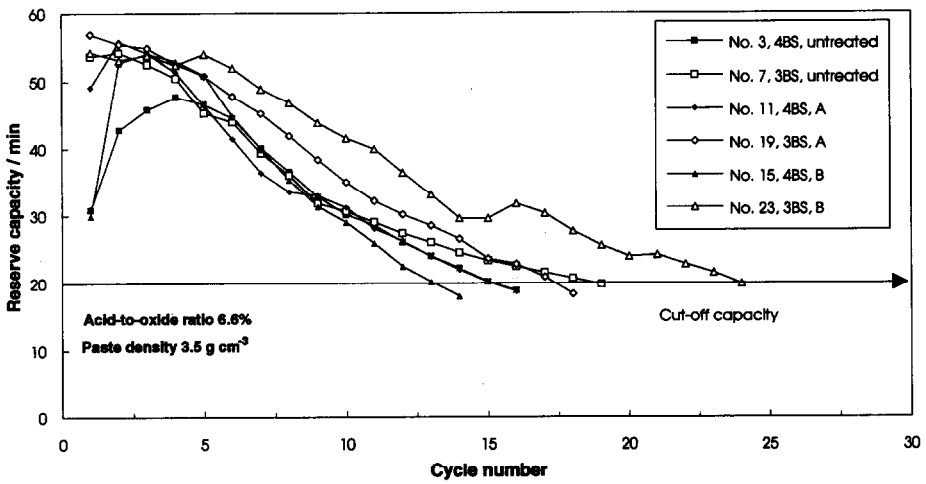

Fig. 16. Repetitive reserve capacity of cells prepared from paste III.

and doped cells, the reserve capacity decreases rapidly after 5 to 10 cycles. For the same paste density of 3.9 g cm^{-3}, the cycleability of both untreated and doped cells increases when the acid-to-oxide ratio employed in paste mixing is reduced from 6.6 to 3.9% (cf., Fig. 14 with Fig. 15). At an acid-to-oxide ratio of either 6.6 or 3.9%, most of the doped cells using 3BS- or 4BS-curing procedures do not exhibit better cycle lives than the corresponding untreated cells (Figs. 14 and 15). Furthermore, the cells produced from 4BS-cured plates generally give inferior performance compared with those using 3BS varieties. A notable exception to this trend is the behaviour of doped cells with 3BS-cured plates prepared from a 3.9% acid-to-oxide ratio. Compared with 4BS counterparts, these cells suffer from a shorter cycle life (Fig. 15).

Similar observations are also made for cells prepared with a lower paste density of 3.5 g cm^{-3} and acid-to-oxide ratios of 6.6 and 3.9% (Figs. 16 and 17), namely:

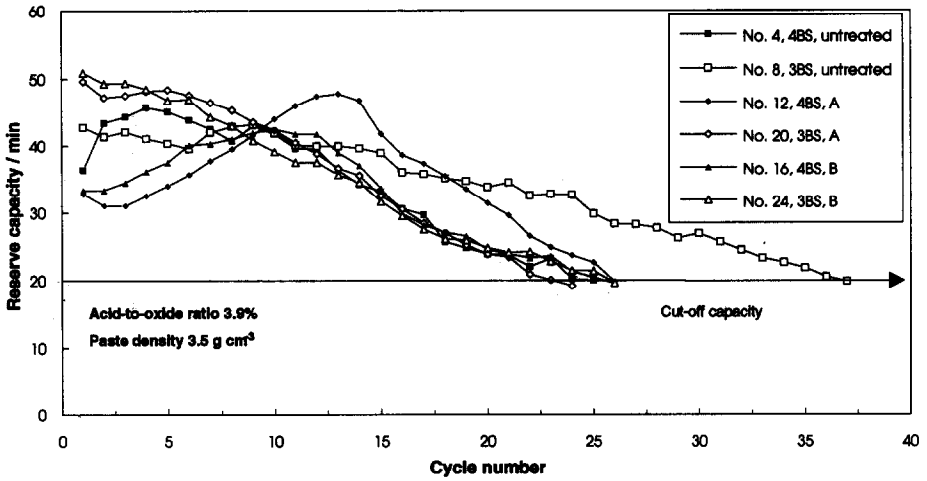

Fig. 17. Repetitive reserve capacity of cells prepared from paste IV.

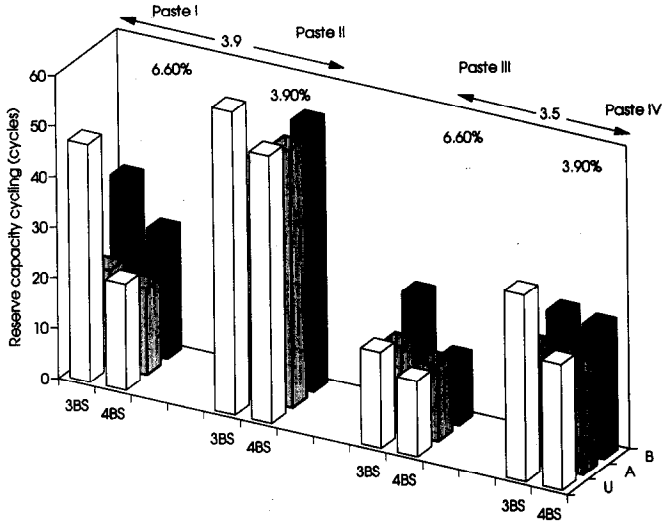

Fig. 18. Schematic representation of repetitive reserve capacity of cells prepared under various conditions; U denotes untreated paste.

(i) the cycleability of both untreated and doped cells increases as the acid-to-oxide ratio decreases; (ii) for the same 4BS- or 3BS-curing procedure, the doped cells display equal, or inferior, performance compared with the corresponding untreated counterparts (except for experiment 23, Fig. 16).

For the same acid-to-oxide ratio (either 6.6 or 3.9%), a decrease in the paste density results in a corresponding decrease in cycle life (Fig. 18).

JIS endurance cycling

The cycle lives of cells (produced from pastes I to IV) under the Japanese Industrial Standard procedure, JIS, are given in Figs. 19 to 22, and summarized

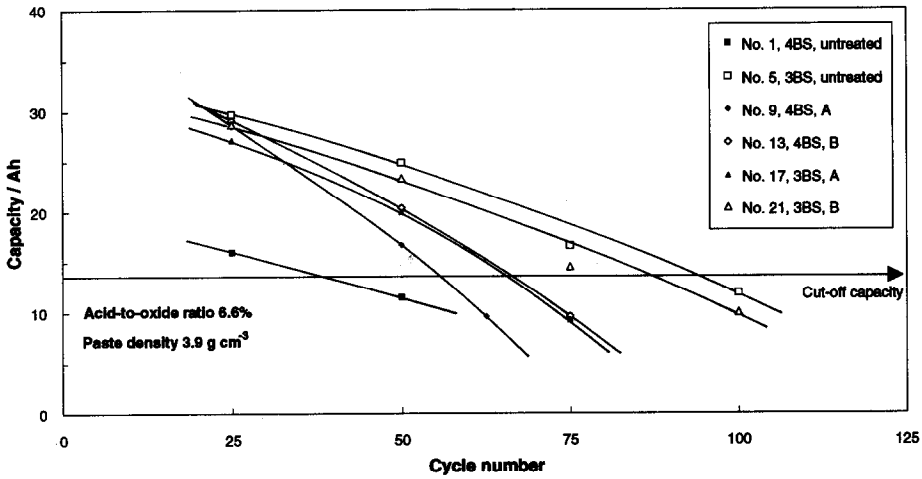

Fig. 19. JIS endurance performance of cells prepared from paste I.

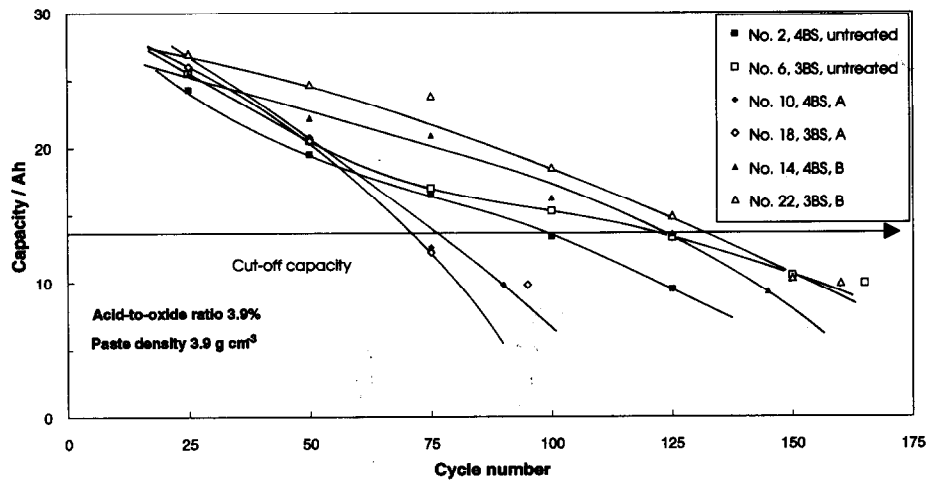

Fig. 20. JIS endurance performance of cells prepared from paste II.

schematically in Fig. 23. Failure, in terms of cycles, is determined by the intersection between the performance curves and a horizontal line drawn at a cutoff capacity of 13.5 Ah. This value is 50% of the nominal 5-h discharge capacity of the cells.

For the same paste density of 3.9 g cm^{-3} (Figs. 19, 20), the cells prepared from 3BS-cured plates using a 6.6 or 3.9% acid-to-oxide ratio and doped with particulate B give a greater cycle life than those cells doped with particulate A. The cycleability of the B-doped cells is virtually the same, or slightly better, than that of untreated cells. Similarly, the B-doped cells prepared from 4BS-cured plates using a 6.6 or 3.9% acid-to-oxide ratio give better performance than either the untreated or A-doped 4BS varieties. As observed above for reserve capacity: (i) the endurance of both untreated and doped cells increases when the acid-to-oxide ratio is decreased; (ii) the performance of cells using 4BS-cured plates is inferior to that of cells made from 3BS-cured plates.

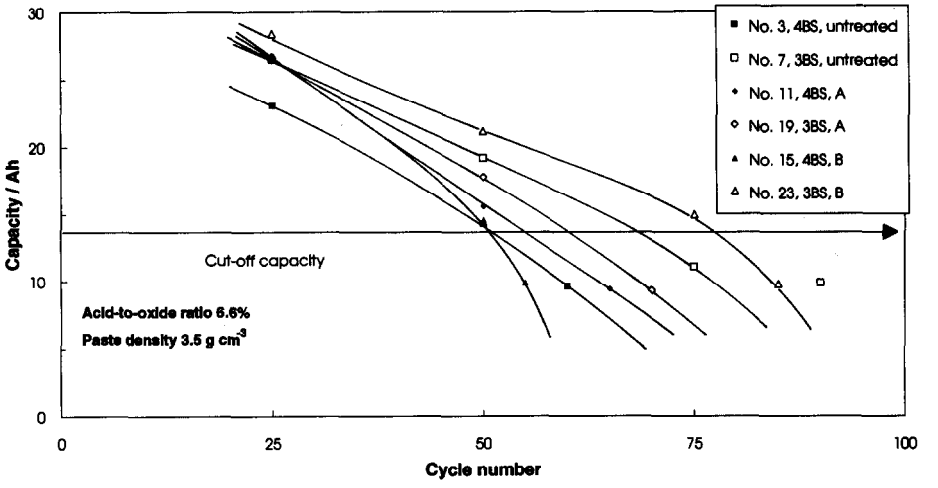

Fig. 21. JIS endurance performance of cells prepared from paste III.

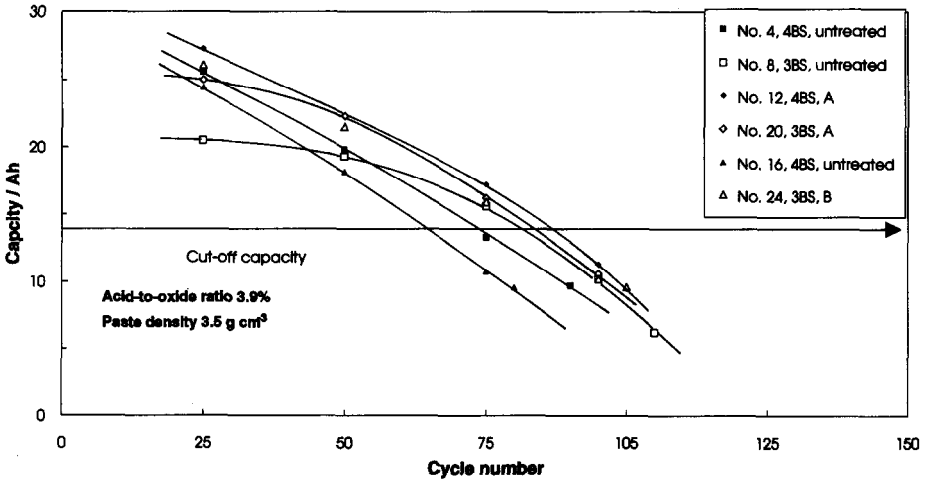

Fig. 22. JIS endurance performance of cells prepared from paste IV.

It should be noted that the 4BS plates used in this study have not been prepared with the advanced curing technique that has been developed in the CSIRO laboratories to give enhanced cycle-life performance under JIS conditions [16].

Similar results are also obtained for cells prepared with a lower paste density of 3.5 g cm^{-3} and acid-to-oxide ratios of 6.6 and 3.9% (Figs. 21, 22), namely: (i) 3BS-cured cells doped with particulate B give greater cycleability than either the untreated or the A-doped cells; (ii) doped 4BS-cured cells display, in general, better performance than untreated varieties.

As observed under reserve-capacity duty, the cycle life decreases with decreasing paste density. This observation holds for an acid-to-oxide ratio of either 6.6 or 3.9% (Fig. 23).

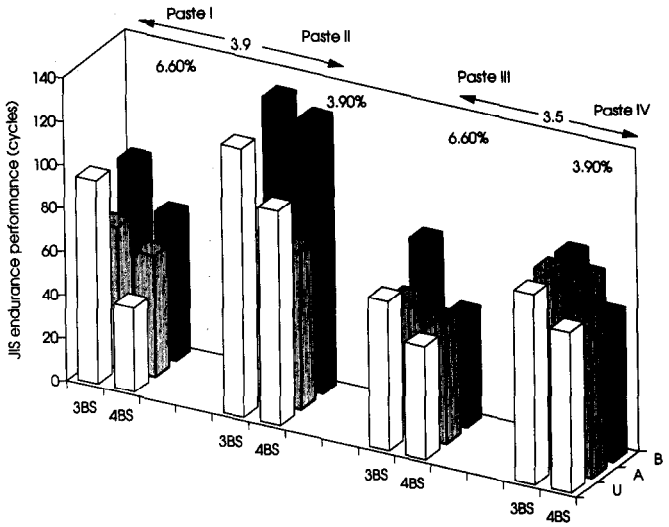

Fig. 23. Schematic representation of JIS endurance performance of cells prepared under various conditions; U denotes untreated paste.

Summary of cell performance

The cycleability of untreated and doped cells under the repetitive reserve capacity and JIS endurance tests is summarized in Table 11. Although the improvement in active-material utilization is about the same when either particulate A or B is added (see Table 9), the cycle life is greater for cells doped with particulate B. Nevertheless, under repetitive reserve-capacity cycling, 4BS-cured plates containing particulate B give, in general, only a slight increase in cycle life compared with the corresponding untreated plates. Furthermore, with 3BS-curing, particulate B invokes an inferior performance. Conversely, under the JIS endurance test, the cells doped with particulate B exhibit significantly better performance than the untreated cells, for both 3BS- and 4BS-curing conditions.

Cell failure mode

The negative plates appear to be in good condition after cell failure under either the repetitive reserve capacity or the JIS procedures. By contrast, the positive plates suffer from a considerable amount of material shedding. This is severe both in the upper regions and at the edges of the plates. Shedding is more advanced in plates that have failed under the JIS endurance test.

After repetitive reserve capacity cycling, failed plates in the discharged state contain lead sulfate crystals of irregular shape and size, i.e., a mixture of large block and small faceted forms, as well as a dendritic form. Small numbers of lead sulfate crystals remain in plates that are in the charged state. The cross-sectional views of the failed plates (in the charged state) reveal two distinct patterns in the corrosion layer (Fig. 24(a)): (i) a dense layer adjacent to the grid; (ii) an outer porous layer with numerous concentric cracks. The outer layer appears very fragile and, therefore, will promote material shedding. Furthermore, the concentric cracks will hinder the flow of electrons to and from the grid during charge and discharge.

Plates that have failed under the JIS endurance test contain, in the discharged state, imperfect lead sulfate crystals. In the charged state, the PbO_2 crystals are found

TABLE 11

Cycle-life performance of untreated and doped cells

Experimental conditions	Performance (cycles)	
	Repetitive reserve capacity	JIS endurance
Paste I: acid-to-oxide ratio = 6.6%; density = 3.9 g cm^{-3}		
5, 3BS, untreated	47	94
17, 3BS, A	19	65
21, 3BS, B	34	88
1, 4BS, untreated	21	39
9, 4BS, A	17	56
13, 4BS, B	25	67
Paste II: acid-to-oxide ratio = 3.9%; density = 3.9 g cm^{-3}		
6, 3BS, untreated	60	124
18, 3BS, A	36	72
22, 3BS, B	44	132
2, 4BS, untreated	53	99
10, 4BS, A	51	73
14, 4BS, B	53	126
Paste III: acid-to-oxide ratio = 6.6%; density = 3.5 g cm^{-3}		
7, 3BS, untreated	19	69
19, 3BS, A	17	62
23, 3BS, B	24	82
3, 4BS, untreated	15	52
11, 4BS, A	15	56
15, 4BS, B	13	52
Paste IV: acid-to-oxide ratio = 3.9%; density = 3.5 g cm^{-3}		
8, 3BS, untreated	37	88
20, 3BS, A	23	91
24, 3BS, B	27	91
4, 4BS, untreated	25	74
12, 4BS, A	26	92
16, 4BS, B	26	67
Failure mode[a]	C	C

[a]C = positive active-material shedding and grid corrosion

to have developed to a larger size, and to be gathered into looser agglomerates, than those present in the initial formed material. The morphology at the grid/active-material interface is different to that observed in plates that had been subjected to repetitive reserve capacity cycling. The corrosion layer in the JIS plates is denser and less fractured (although a few radial cracks are observed, see Fig. 24(b)). In addition, there is a good contact both between the corrosion layer and the active material, and between the material and the conductive glass-flakes.

In summary, the failure of the cells under the above two test procedures is due to shedding of positive active material, together with extensive grid corrosion. Under repetitive reserve capacity cycling, the failure mode appears to be determined by the development of a fragile, outer corrosion layer that introduces electrical conductivity losses and encourages shedding of active material. By contrast, the failure mode under

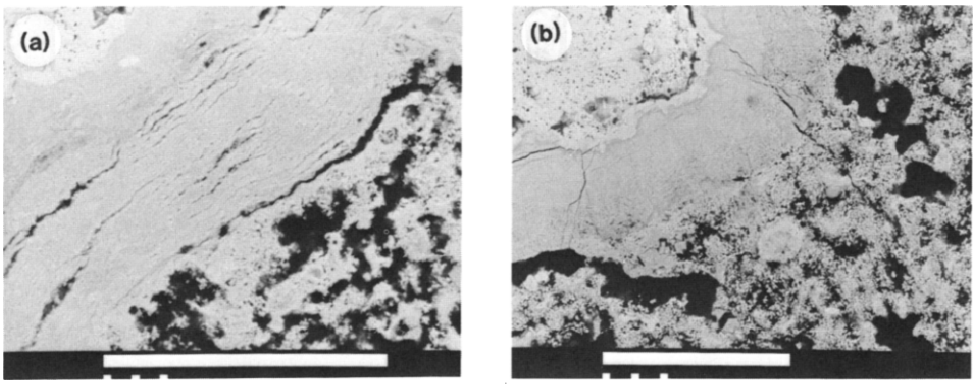

Fig. 24. Cross sections of failed positive plates in a charged state after (a) repetitive reserve capacity test, and (b) JIS endurance test; magnification bar: 100 μm.

the JIS endurance test appears to arise from a general 'softening' of the active material itself. This is probably the result of the continuous overcharge that is applied in the test (the charge/discharge ratio on each cycle under the JIS profile is 125%).

Conclusions

The objective of this project has been to determine the effect of conductive glass-flakes on the active-material utilization and related performance characteristics of plate materials produced under different acid-to-oxide ratios, paste densities, and curing conditions. From the above observations, the following conclusions can be drawn.

(i) The conductive coating of both particulates A and B consists mainly of tin dioxide. The layer has an uneven thickness that varies between 0.3 and 5 μm. At certain locations, the glass-flake substrate is completely exposed. This suggests that both the coverage and the throwing power of the tin dioxide coating require improvement. Compared with particulate A, particulate B has smaller grains of tin dioxide and a higher stability in acid.

(ii) Doping with tin-dioxide-coated glass-flake produces little effect on either the morphology or the phase composition of the pasted materials. It does, however, influence the nucleation and growth of 4BS crystals during curing; the size of these crystals is reduced. Nevertheless, the acid-to-oxide ratio is found to be the main factor that affects the level and size of the 3BS and 4BS crystals in either the paste or the cured materials: the yields of 3BS and 4BS decrease, the size of 3BS increases, and the size of 4BS decreases, when using a low acid-to-oxide ratio. A strong interlock exists between the active-material/grid member and the active-material/glass-flakes after both the curing and formation processes.

(iii) Both additives are found to assist the formation process and to increase the BET surface area, but to give no major overall improvement in porosity or pore volume.

(iv) Active-material utilization is increased through the addition of glass-flakes when cells are discharged at either the 20-h or the 5-h rate. The improvement becomes greater when the paste density is decreased from 3.9 to 3.5 g cm^{-3}, namely, $\sim$4 to 14% compared with $\sim$2 to 31%.

(v) The addition of conductive glass-flake provides no benefits in terms of enhanced cold-cranking performance.

(vi) Under repetitive reserve capacity cycling, 4BS-cured plates containing particulate B display a slight increase in cycleability compared with corresponding untreated plates. No advantageous effects are observed with particulate A. With 3BS-curing conditions, both particulates A and B invoke inferior performance.

(vii) Under JIS endurance test conditions, cells doped with particulate B yield better performance than untreated cells made from either 3BS- or 4BS-cured plates.

(viii) Overall, particulate B is more beneficial than particulate A. This is probably related to the greater dimension and stability of particulate B.

(ix) For all test schedules, the cell failure occurs through the combined effects of grid corrosion and shedding of active material in the positive plates. Under repetitive reserve-capacity cycling, the failure mode is predominantly governed by the development of an outer fragile corrosion layer, that both provides a barrier to electron flow during the charge/discharge reactions and destabilizes the active material. By contrast, the failure mode under the more severe overcharge action of the JIS endurance test is associated mainly with a general degradation of the structure of the positive material itself.

Acknowledgements

The authors are grateful to the Monsanto Chemical Company for supporting this work and for granting permission to publish the outcomes. Special thanks are due to Mr Martin Wohl, Manager of Business Development, Monsanto Chemical Company for helpful discussions. The authors are also indebted to the Automotive Division of GNB Australia and its Process Engineer, Mr Gregory Constantinou, for supplying the battery materials used in this investigation.

References

1 H. Dietz, J. Garche and K. Wiesener, *J. Power Sources, 14* (1985) 305.
2 A. Tokunaga, M. Tsubota, K. Yonazu and K. Ando, *J. Electrochem. Soc., 134* (1987) 525.
3 S.V. Baker, P.T. Moseley and A.D. Turner, *J. Power Sources, 27* (1989) 127.
4 D.B. Edwards and V.S. Srikanth, *J. Power Sources, 34* (1991) 217.
5 J.L. Weininger and C.R. Morelock, *J. Electrochem. Soc., 122* (1975) 1161.
6 W.-H. Kao and K.R. Bullock, *J. Electrochem. Soc., 139* (1992) L41.
7 N.E. Bagshaw, R.L. Clarke and K. Kendall, *Ext. Abstr., Proc. Fall Meet. Electrochemical Society, Seattle, WA, USA, Oct. 14–19, 1990,* Vol. 90-2, p. 2.
8 T.J. Clough, *Proc. 24th Intersoc. Energy Conversion Engineering Conf., Washington, DC, USA, Aug. 6–11, 1989,* Vol. 4, p. 1857.
9 L.T. Lam, H. Ozgun, L.M.D. Cranswick and D.A.J. Rand, *J. Power Sources, 42* (1993) 55.
10 R.J. Hill, A.M. Foxworthy and R.J. White, *J. Power Sources, 32* (1990) 315.
11 G.L. Corino, R.J. Hill, A.M. Jessel, D.A.J. Rand and J.A. Wunderlich, *J. Power Sources, 16* (1985) 141.
12 Lead/Acid Batteries, *Australian Standard AS 2149-1985.*
13 Lead/Acid Batteries for Automobiles, *Japanese Industrial Standard JIS D 5301-1986.*
14 T.G. Chang, *J. Electrochem. Soc., 131* (1984) 1755.
15 D. Pavlov and E. Bashtavelova, *J. Electrochem. Soc., 133* (1986) 241.
16 D.A.J. Rand and L.T. Lam, *The Battery Man,* (Nov.) (1992) pp. 18–22, 24, 27, 28.